Original Article
pISSN 1738-2637 / eISSN 2288-2928
J Korean Soc Radiol 2016;74(3):160-168
http://dx.doi.org/10.3348/jksr.2016.74.3.160

대한영상의학회지

Assessment of Carotid Diffusion-Weighted Imaging for Detection of Lipid-Rich Necrotic Core in Symptomatic Carotid Atheroma

경동맥 확산강조영상으로 증상이 있는 경동맥 죽종의 지방 풍부 괴사핵을 발견할 수 있는가?

Kang Ji Lee, MD[1], Hyo Sung Kwak, MD[1,2]*, Gyung Ho Chung, MD[1], Seung Bae Hwang, MD[1], Ji Soo Song, MD[1]

[1]Department of Radiology, Chonbuk National University Hospital and Medical School, Jeonju, Korea
[2]Radiology and Research Institute of Clinical Medicine of Chonbuk National University-Biomedical Research Institute of Chonbuk National University Hospital, Jeonju, Korea

Purpose: To evaluate the diagnostic usefulness of diffusion-weighted MR imaging (DWI) compared with contrast-enhanced MR imaging for the detection of the lipid-rich necrotic core (LRNC) of symptomatic carotid atherosclerotic plaques.

Materials and Methods: Twenty-five patients (median age: 66 years; range: 45–78 years) with moderate-to-severe symptomatic carotid stenosis confirmed with contrast-enhanced carotid MR angiography who underwent carotid plaque MR imaging were retrospectively reviewed. An echo-planner DWI with b0, b200, b400, b800, and b1000 was performed along with carotid plaque MR imaging. Plaque visualization on DWI was analyzed by 2 reviewers on consensus. The contrast-to-noise ratio between the lumen and plaque was analyzed between variable b-values.

Results: Carotid atherosclerotic plaques were identified on carotid DWI in 8 patients. Confirmed carotid atherosclerotic plaques were not identified on carotid DWI in 16 patients. The DWI-identified group had plaques with significantly greater maximal wall thickness and longitudinal length, as compared with the non-identified group. DWI with b200 had a higher contrast-to-noise ratio between the lumen and LRNC ($p < 0.001$). The mean apparent diffusion coefficient value from DWI with b200 for the LRNC was $0.51 \pm 1.55 \times 10^{-3}$ mm^2/s.

Conclusion: There was less frequent identification of carotid atherosclerotic plaques with carotid DWI, as compared with contrast-enhanced MR imaging. This study suggested that carotid DWI cannot replace contrast-enhanced MR imaging for the detection of carotid plaques, including LRNC.

Index terms
Carotid Artery Disease
Carotid Stenosis
Plaque, Atherosclerotic
Magnetic Resonance Angiography
Diffusion Weighted MRI

Received June 25, 2015
Revised September 25, 2015
Accepted October 13, 2015
***Corresponding author:** Hyo Sung Kwak, MD
Radiology and Research Institute of Clinical Medicine of Chonbuk National University-Biomedical Research Institute of Chonbuk National University Hospital, 20 Geonji-ro, Deokjin-gu, Jeonju 54907, Korea.
Tel. 82-63-250-2582 Fax. 82-63-272-0481
E-mail: kwak8140@jbnu.ac.kr

INTRODUCTION

Atherosclerosis is a disease in which plaque builds up inside the arteries. Hardening of plaques with consequent narrowing of arteries can lead to serious problems, including heart attack, stroke, or even death. In particular, if plaques build up in the carotid arteries, blood flow to the brain can be reduced or blocked by ruptured plaque or embolization, potentially leading to stroke. The progression of carotid atherosclerosis can be attributed to systemic factors such as age, sex, and statin therapy, as well as local factors such as intraplaque hemorrhage (IPH), ulcers, and thin fibrous caps (1-6). Complex carotid plaques with IPH, ulcers, or thin-fibrous caps are associated with the occurrence of subsequent cerebrovascular events (7-9). In particular, IPH into the carotid atherosclerotic plaque is significantly associated with more rapid progression of plaque size and lipid-rich necrotic core (LRNC), as well as luminal stenosis (4).

High-resolution MRI is a proven noninvasive imaging tool

with excellent capability for discriminating tissues of the carotid plaque, including the status of the fibrous cap, LRNC, calcium, and hemorrhage (10-14). Previous studies have applied conventional spin echo diffusion-weighted imaging (DWI) for diagnosis of the disease (15-17). The lower apparent diffusion coefficient (ADC) values in the intraplaque lipid and hemorrhage than the normal carotid wall, suggest their substantial value in plaque component discrimination (16). DWI may help stratify patients according to risk of carotid atherosclerosis and thus, selection of appropriate treatment. However, these studies did not compare carotid DWI and contrast-enhanced carotid MR imaging for the evaluation of LRNC.

We hypothesized that carotid DWI for the diagnosis of LRNC may have a similar diagnostic value, as compared with contrast-enhanced carotid MR imaging. Therefore, we comparatively evaluated the diagnostic usefulness of carotid DWI and contrast-enhanced MR imaging for the detection of LRNC in symptomatic carotid atherosclerotic plaques.

MATERIALS AND METHODS

Patient Recruitment

The study was approved by the local Institutional Review Board and informed consent was obtained from all patients before imaging. Between August 2013 and February 2014, we reviewed data on consecutive patients with > 50% symptomatic stenosis of unilateral carotid arteries on contrast-enhanced carotid MR angiography who underwent carotid-plaque MR imaging including DWI and contrasted-enhanced imaging, retrospectively. Symptomatic carotid artery stenosis was defined as the onset of focal neurologic symptoms [transient ischemic attack (TIA) or nonfatal stroke] occurring within 6 months of carotid plaque MR imaging and attributable to an ipsilateral carotid artery vascular distribution. Exclusion criteria were poor image quality by MR imaging, insufficient coverage (< 10 mm including the bifurcation), LRNC with IPH, or prior radiation therapy to the neck.

MR Imaging Protocol

Carotid MR imaging was performed on a 3T MRI scanner (Achieva; Philips Medical Systems, Best, the Netherlands) with a 16 channel head coil. A standardized multicontrast protocol for carotid MR imaging was used to obtain three-dimensional (3D) time of flight angiography, two-dimensional (2D) T1-weighted black blood images, T2-weighted black blood images, 3D magnetization-prepared rapid acquisition with gradient-echo (MPRAGE) black blood images, diffusion-weighted imaging, and contrast-enhanced MR imaging (18, 19). For contrast-enhanced MR imaging, a contrast-agent (Dotarem; Guerbet, Aulnay-sous-Bois, France; 0.1 mmol/kg body weight) was injected intravenously with a power injector, and post-contrast T1-weighted images were acquired 5 minutes after injection. All 2D images were obtained with a field of view (FOV) of 14 cm and matrix size of 256 × 256 with 2 signal-intensity averages, and were acquired with a 2-mm section thickness for a total longitudinal coverage of 20−24 mm centered at the bifurcation of the atherosclerotic artery. 3D images were acquired with 1-mm section thickness. Total acquisition time for all images was approximately 30−40 minutes.

The imaging parameters in DWI were: receiver bandwidth = 1086 kHz/pixel, FOV = 140 × 140, imaging matrix = 84 × 80, 2.0 mm slice thickness, effective echo time = 84 ms, repetition time = 1768 ms, 43 echoes per slice, b = 0, b = 200, b = 400, b = 800, and 1000 s/mm^2 along the slice selection direction, 32 averages (magnitude) at each b-value and of 16 contiguous slices were obtained. The in-plane spatial resolution for typical data acquisition was 1 × 1 mm^2 with a display resolution 0.5 × 0.5 mm^2 after zero-filled interpolation. The total imaging time for 16 slices with 32 averages of both b-values was approximately 3 minutes. A multishot diffusion-weighted echo-planar imaging (EPI) sequence was used to obtain DW images (b = 0, b = 200, b = 400, b = 800, and b = 1000 s/mm^2). Diffusion gradients were applied in turn to the x, y, and z axes. A mean DW image was then computed for the x, y, and z-prepared diffusion images. Saturation bands were positioned superiorly and inferiorly to suppress signal from inflowing blood and anteriorly and posteriorly to minimize wrap-around artifact.

Image Analysis

We used contrast-enhanced MR imaging as the gold standard of diagnostic accuracy of DWI for the evaluation of LRNC (20). Initially, the image-quality rating (4-point scale: 1 = poor, 4 = excellent) for contrast-enhanced MR imaging and DWI was decided by consensus opinion of 2 reviewers (neuroradiologists with 20 and 7 years of experience). For images with imaging quality

rating ≥ grade 2, image analysis software (MRI-Plaqueview; VP Diagnostics, Seattle, WA, USA) was used to draw the lumen and outer wall boundaries. The maximal wall thickness and longitudinal length of the plaque on contrast-enhanced MR imaging were measured by reviewers reaching a consensus opinion.

We used a 4-point grading system to assess the clarity of the plaque margin on DWI by 2 reviewers; grade 0, unidentifiable plaque; grade 1, plaque with ill-defined margins; grade 2, plaque with well-defined margins; grade 3, definite visualization of the plaque. We dichotomized this grading system into the identification (grade 2 and 3) or lack of identification (grade 0 and 1) of carotid plaques on DWI. We calculated the contrast-to-noise ratios (CNR, where CNR = S_{LRNC} - S_{lumen} / S_{noise}) for each b-value for slices with maximal wall thickness on DWI in patients with plaque margins ≥ grade 2. The mean signal measurements for the ROIs were recorded, and standard deviation measurements were defined (S_{noise}) using ROIs drawn in a peripheral area of the image uncontaminated by artifact.

The ADC of the LRNC for b-values with high CNR was automatically calculated by the MR system and displayed as the cor-

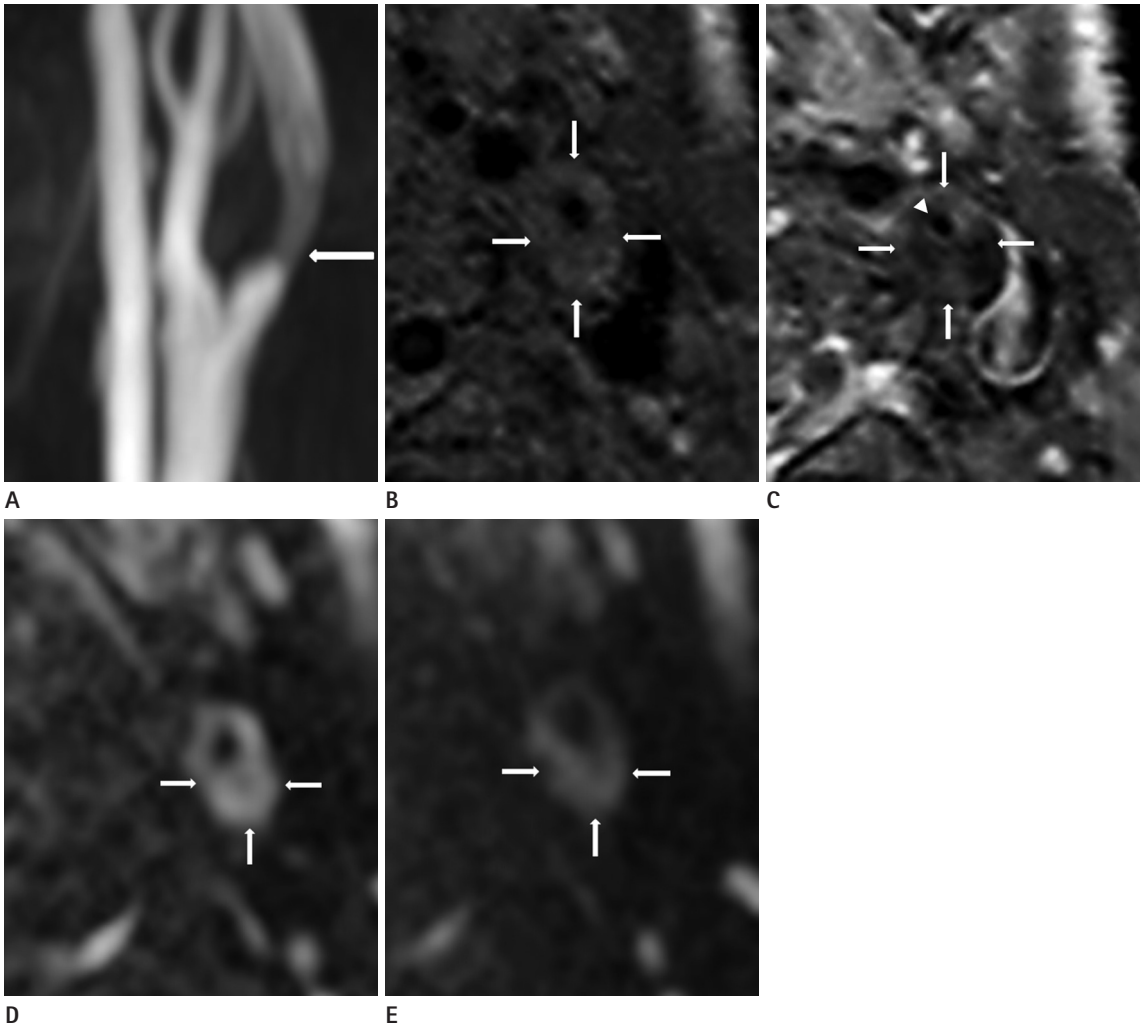

Fig. 1. A 76-year-old man with left symptomatic carotid stenosis (case 4).
A. TOF MR angiography shows an eccentric plaque of the left proximal internal carotid artery (arrow).
B. Axial T1-weighted imaging shows a circumferential plaque (arrows). Maximal wall thickness is 8.2 mm and the longitudinal length of plaque is 26 mm.
C. Black-blood contrast-enhanced MR imaging shows large LRNC (arrows) with thin/ruptured fibrous cap (arrowhead).
D. DWI with b 200 s/mm^2 shows high signal intensity with similar area of contrast-enhanced MR imaging (arrows). Contrast-to-noise ratio: 34.31 mm^2/s.
E. DWI with b 1000 s/mm^2 shows low signal intensity, as compared with b 200 s/mm^2.
DWI = diffusion-weighted imaging, LRNC = lipid-rich necrotic core, TOF = time of flight

responding ADC map.

Statistical Analysis

The paired *t*-test was used to compare categorical variables between contrast-enhanced MR imaging and DWI and the CNR of the LRNC and lumen between each b-value. *p*-values < 0.05 were considered statistically significant. All statistical analysis was performed using R 2.14.1 (R Foundation for Statistical Computing, Vienna, Austria).

RESULTS

Patients

Thirty-one consecutive patients with > 50% symptomatic carotid stenosis underwent plaque MR imaging including contrast-enhanced imaging and carotid DWI. Of these patients, 2 had poor image quality, 2 had insufficient coverage, and 3 had IPHs. Therefore, 24 patients (median age: 66 years; range: 45–78 years) were enrolled in this study.

Plaque Visualization of DWI

Of the 24 patients, only 8 patients (33.3%) had plaque margins > grade 2 on DWI. Twelve patients did not show plaque (grade 0) and 4 had grade 1 plaque margins on DWI. The maximal wall thickness of the identified group of carotid plaque on carotid DWI was significantly higher than that of the non-identified group (7.12 ± 1.96 vs. 4.55 ± 0.41, $p < 0.001$) (Fig. 1). The length of the plaques of the identified group on carotid DWI was significantly greater than that of the non-identified group (22.6 ± 3.3 vs. 18.4 ± 3.5, $p < 0.01$) (Fig. 2).

Contrast–to–Noise Ratio of b–Values

The CNR between the LRNC and lumen of each b-value was shown in Table 1. The best CNR between the LRNC and lumen can be achieved when the b-value is set to 200 ($p < 0.001$) (Fig. 3). The mean ADC value from DWI with b200 in LRNC was 0.51 ± 1.55 × 10^{-3} mm^2/s.

DISCUSSION

This study was the first to evaluate the clinical usefulness of carotid DWI compared with contrast-enhanced MR imaging for the diagnosis of LRNC. The results indicated that the carotid plaque margin of DWI had a lower prevalence compared with that of contrast-enhanced MR imaging. The identified group on carotid DWI had a significantly greater maximal wall thickness and longitudinal length of the plaque, as compared with the non-identified group.

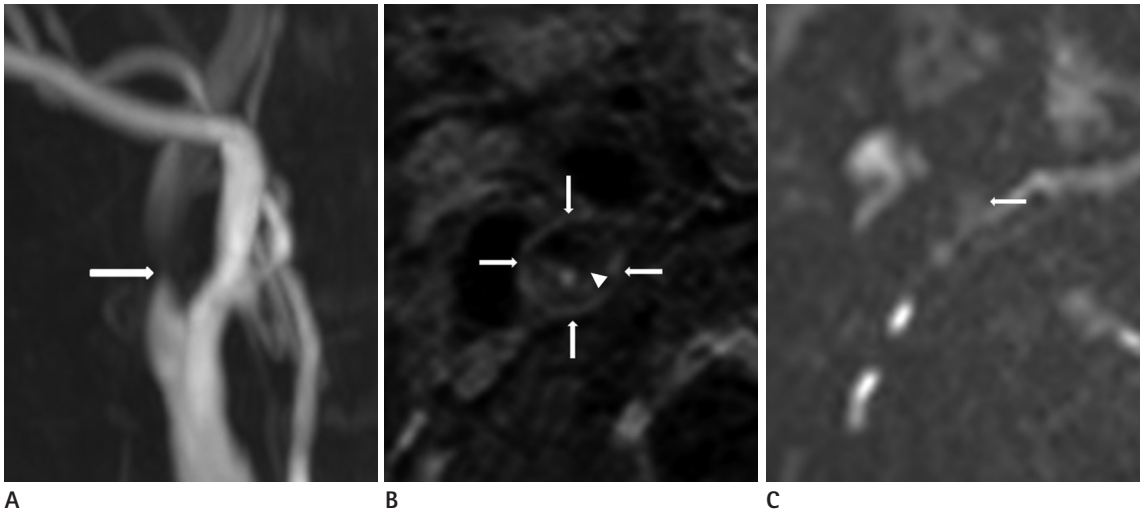

Fig. 2. A 78-year-old man with right symptomatic carotid stenosis.
A. TOF MR angiography shows an eccentric plaque of the right proximal internal carotid artery (arrow). Maximal wall thickness is 5.2 mm and the longitudinal length of the plaque is 16 mm.
B. Black-blood contrast-enhanced MR imaging shows large LRNC (arrows) with thin/ruptured fibrous cap (arrowhead).
C. DWI with b 200 s/mm^2 shows an ill-defined margin of carotid plaque due to partial volume artifact (arrow).
DWI = diffusion-weighted imaging, LRNC = lipid-rich necrotic core, TOF = time of flight

Table 1. Contrast-to-Noise Ratio of Each b-Value of the DWI-Identified Groups (s/mm²)

Number	b = 0	b = 200	b = 400	b = 800	b = 1000
1	34.63	36.74	22.84	8.78	3.62
2	20.94	23.32	17.98	4.32	3.51
3	7.89	15.95	21.5	9.38	8.74
4	7.29	7.73	6.17	5.05	2.81
5	25.34	34.31	20.84	7.05	3.84
6	21.84	22.05	16.94	5.23	4.25
7	7.89	15.95	21.5	9.38	8.74
8	14.52	17.33	12.21	6.32	2.48
Mean	17.54	21.67	17.50	6.94	4.75
SD	9.88	9.77	5.71	2.04	2.53

DWI = diffusion-weighted imaging, SD = standard deviation

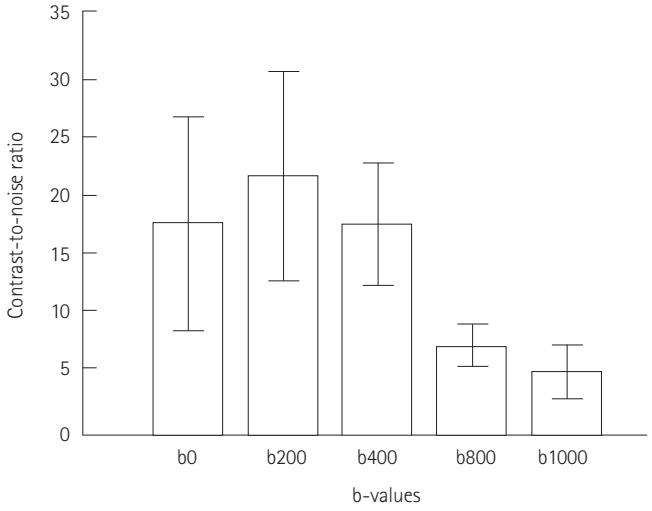

Fig. 3. Contrast-noise ratio of each b-value in the DWI-identified group. DWI = diffusion-weighted imaging

A carotid MR classification of plaques is modified from the American Heart Association (AHA) grading system. A type IV/V plaque describes "vulnerable" plaques with a large lipid core, whereas an AHA type VI plaque exhibits features consistent with acute events, as suggested by IPHs, cap ruptures, or thrombi (21). Carotid MR imaging in patients experiencing minor stroke and TIA showed a higher proportion of type VI complex plaques, as compared with asymptomatic controls (8, 22). Takaya et al. (4) reported that among patients who initially had asymptomatic 50% to 79% carotid stenosis, arteries with thinned or ruptured fibrous caps, IPH, larger maximum % LRNC, and larger maximum wall thickness by MRI were associated with subsequent cerebrovascular events. Therefore, the early detection of IPH as well as accurate diagnosis of LRNC and the fibrous cap status is very important on carotid MR imaging.

The development of IPH poses an immediate and long-term effect on plaque progression and alters the biology and material history of carotid atherosclerosis (5, 6). Intensive lipid therapy significantly depletes LRNC without IPH (2). Regression in overall plaque burden was observed primarily at locations with a LRNC. The detection of IPH by MR imaging primarily relies on the identification of methemoglobin, which is an oxidation product of hemoglobin. Methemoglobin can significantly shorten T1 relaxation and consequently generate a bright signal on T1-weighted images (23). Several studies already introduced MR sequencing such as MPRAGE and slab-selective phase-sensitive inversion-recovery for the detection of IPH (24-26). However, the diagnosis of LRNC in gadolinium-based, contrast-enhanced MR imaging is through the discrimination of the fibrous cap from the LRNC (14, 20, 27). Yuan et al. (14) showed that the enhancement of fibrous tissue was moderate-to-strong (79.5 ± 29.1%), whereas the LRNC enhanced only slightly (28.8 ± 20.1%). Wasserman et al. (27) showed that the CNR was as good as or better than those obtained with T2-weighted MR images, but had approximately twice the signal-to-noise ratio (SNR). Recently, some studies have reported on the usefulness of carotid DWI for the evaluation of plaque burden and composition (15-17).

In previous DWI studies on *ex vivo* specimens, higher b-values (usually 1000 s/mm²) were used to create ADC maps (28, 29). The results of our study indicated that the best CNR between the LRNC and the lumen is achieved when the b-value is set to 200 s/mm². The diffusion-weighted gradient echo is typically several tens-of-milliseconds in length, which inevitably leads to longer TE. This long TE results in T2 signal decay and reduced SNR in the *in vivo* DWI of the carotid artery from which the ADC is cal-

culated (16). Recently, studies have used a b-value of 300 s/mm^2 to obtain ADC maps with reasonable SNR (15, 16).

Young et al. (17) reported the usefulness of DWI for the detection of LRNC in carotid atheroma *in vivo*. The mean ADC values were significantly different between the fibrous cap and LRNC (1.0×10^{-3} mm^2/s vs. 0.7×10^{-3} mm^2/s). Therefore, they suggested that carotid DWI has potential benefit for the detection of the LRNC. Kim et al. (16) reported that the mean ADC values of the carotid plaque components *in vivo* are consistent with values obtained from *ex vivo* endarterectomy specimens. The mean ADC values obtained from the *in vivo* DWI in the normal vessel wall, LRNC, and hemorrhage were 1.27 ± 0.16, 0.38 ± 0.1, and 0.98 ± 0.25×10^{-3} mm^2/s, respectively. In our study, the mean ADC value of the LRNC was 0.51 ± 1.55×10^{-3} mm^2/s. This value was similar to that of previous studies (16, 17).

Kim et al. (15) reported partial visualization of the carotid wall on all ADC images, but full visualization on only 18% of images (6/33). In our study, only 33% of the images had clear plaque margins > grade 2 on carotid DWI, and we could not obtain the ADC maps of 8 patients. The remaining patients (16/24) had unidentified plaques or plaques with ill-defined margins. The maximal wall thickness of the DWI-identified group of carotid plaques was significantly higher than that of the non-identified group, with significantly greater longitudinal length of the plaques on DWI in the identified group, as compared to the non-identified group. This finding suggests that if carotid atheroma have smaller wall thicknesses and short segment lengths, carotid DWI cannot be used to analyze plaque volume. The lower resolution of carotid DWI *in vivo* is likely attributable to a greater partial volume effect. A given component is affected by the partial volume effect based upon its spatial distribution within the plaque and the number of other adjacent tissues (4). Therefore, we used the multi-shot EPI technique that improves spatial resolution while minimizing artifacts and maintaining SNR. However, carotid DWI had a limited role because of poor spatial resolution.

DWI has an advantage of not requiring the use of gadolinium-based contrast agents. Contrast-enhanced T1-weighted imaging is becoming the most popular method for differentiating fibrous cap and LRNC, however, it is not desirable in some subgroups of patients, for example, those with allergies and renal disease. We agree with Young et al. (17) that although carotid DWI cannot effectively distinguish LRNC from other plaque components, improvements in image quality may be expected in the future.

Our study had several limitations. The primary limitation was the small sample number that prevented any definitive conclusion on the accuracy of DWI. The study, however, is valuable as a preliminary study. Another limitation was the lack of a gold standard histological reference. Cai et al. (20) performed a comparison of high-resolution, contrast-enhanced MR imaging and histology for the quantitative measurement of intact fibrous caps and LRNC in atherosclerotic carotid plaques. Quantitative measurements of fibrous cap length along the lumen circumference, fibrous cap area, and LRNC area were collected from contrast-enhanced MR imaging and histology sections. Therefore, we considered the non-enhancing areas on carotid contrast-enhanced MR imaging as strongly supportive of the presence of LRNC.

In conclusions, the early results indicated that it is difficult to differentiate LRNCs from carotid atheroma with short segments and small plaque volumes using DWI. However, LRNC with large volumes and diffusion restriction in DWI show appreciable differences. In addition, for LRNC assessment, acquiring b = 200 image improves the accuracy of the DWI measurement in the *in vivo* human carotid artery. Thus, DWI for the differential detection of LRNC from carotid plaques cannot replace contrast-enhanced MR imaging because of poor imaging quality.

Acknowledgments

Financial support for the publication of this study was provided by TAEJOON PHARM Co., Ltd./ACCUZEN, Seoul, South Korea.

REFERENCES

1. Smilde TJ, van Wissen S, Wollersheim H, Trip MD, Kastelein JJ, Stalenhoef AF. Effect of aggressive versus conventional lipid lowering on atherosclerosis progression in familial hypercholesterolaemia (ASAP): a prospective, randomised, double-blind trial. *Lancet* 2001;357:577-581
2. Zhao XQ, Dong L, Hatsukami T, Phan BA, Chu B, Moore A, et al. MR imaging of carotid plaque composition during lipid-lowering therapy a prospective assessment of effect and time course. *JACC Cardiovasc Imaging* 2011;4:977-986
3. Migrino RQ, Bowers M, Harmann L, Prost R, LaDisa JF Jr.

Carotid plaque regression following 6-month statin therapy assessed by 3T cardiovascular magnetic resonance: comparison with ultrasound intima media thickness. *J Cardiovasc Magn Reson* 2011;13:37
4. Takaya N, Yuan C, Chu B, Saam T, Polissar NL, Jarvik GP, et al. Presence of intraplaque hemorrhage stimulates progression of carotid atherosclerotic plaques: a high-resolution magnetic resonance imaging study. *Circulation* 2005;111:2768-2775
5. Sun J, Underhill HR, Hippe DS, Xue Y, Yuan C, Hatsukami TS. Sustained acceleration in carotid atherosclerotic plaque progression with intraplaque hemorrhage: a long-term time course study. *JACC Cardiovasc Imaging* 2012;5:798-804
6. Sun J, Balu N, Hippe DS, Xue Y, Dong L, Zhao X, et al. Subclinical carotid atherosclerosis: short-term natural history of lipid-rich necrotic core--a multicenter study with MR imaging. *Radiology* 2013;268:61-68
7. Takaya N, Yuan C, Chu B, Saam T, Underhill H, Cai J, et al. Association between carotid plaque characteristics and subsequent ischemic cerebrovascular events: a prospective assessment with MRI--initial results. *Stroke* 2006;37:818-823
8. Parmar JP, Rogers WJ, Mugler JP 3rd, Baskurt E, Altes TA, Nandalur KR, et al. Magnetic resonance imaging of carotid atherosclerotic plaque in clinically suspected acute transient ischemic attack and acute ischemic stroke. *Circulation* 2010;122:2031-2038
9. Turc G, Oppenheim C, Naggara O, Eker OF, Calvet D, Lacour JC, et al. Relationships between recent intraplaque hemorrhage and stroke risk factors in patients with carotid stenosis: the HIRISC study. *Arterioscler Thromb Vasc Biol* 2012;32:492-499
10. Toussaint JF, LaMuraglia GM, Southern JF, Fuster V, Kantor HL. Magnetic resonance images lipid, fibrous, calcified, hemorrhagic, and thrombotic components of human atherosclerosis in vivo. *Circulation* 1996;94:932-938
11. Shinnar M, Fallon JT, Wehrli S, Levin M, Dalmacy D, Fayad ZA, et al. The diagnostic accuracy of ex vivo MRI for human atherosclerotic plaque characterization. *Arterioscler Thromb Vasc Biol* 1999;19:2756-2761
12. Fayad ZA, Fuster V. Characterization of atherosclerotic plaques by magnetic resonance imaging. *Ann N Y Acad Sci* 2000;902:173-186
13. Yuan C, Mitsumori LM, Ferguson MS, Polissar NL, Echelard D, Ortiz G, et al. In vivo accuracy of multispectral magnetic resonance imaging for identifying lipid-rich necrotic cores and intraplaque hemorrhage in advanced human carotid plaques. *Circulation* 2001;104:2051-2056
14. Yuan C, Kerwin WS, Ferguson MS, Polissar N, Zhang S, Cai J, et al. Contrast-enhanced high resolution MRI for atherosclerotic carotid artery tissue characterization. *J Magn Reson Imaging* 2002;15:62-67
15. Kim SE, Jeong EK, Shi XF, Morrell G, Treiman GS, Parker DL. Diffusion-weighted imaging of human carotid artery using 2D single-shot interleaved multislice inner volume diffusion-weighted echo planar imaging (2D ss-IMIV-DWEPI) at 3T: diffusion measurement in atherosclerotic plaque. *J Magn Reson Imaging* 2009;30:1068-1077
16. Kim SE, Treiman GS, Roberts JA, Jeong EK, Shi X, Hadley JR, et al. In vivo and ex vivo measurements of the mean ADC values of lipid necrotic core and hemorrhage obtained from diffusion weighted imaging in human atherosclerotic plaques. *J Magn Reson Imaging* 2011;34:1167-1175
17. Young VE, Patterson AJ, Sadat U, Bowden DJ, Graves MJ, Tang TY, et al. Diffusion-weighted magnetic resonance imaging for the detection of lipid-rich necrotic core in carotid atheroma in vivo. *Neuroradiology* 2010;52:929-936
18. Yuan C, Kerwin WS, Yarnykh VL, Cai J, Saam T, Chu B, et al. MRI of atherosclerosis in clinical trials. *NMR Biomed* 2006;19:636-654
19. Underhill HR, Yarnykh VL, Hatsukami TS, Wang J, Balu N, Hayes CE, et al. Carotid plaque morphology and composition: initial comparison between 1.5- and 3.0-T magnetic field strengths. *Radiology* 2008;248:550-560
20. Cai J, Hatsukami TS, Ferguson MS, Kerwin WS, Saam T, Chu B, et al. In vivo quantitative measurement of intact fibrous cap and lipid-rich necrotic core size in atherosclerotic carotid plaque: comparison of high-resolution, contrast-enhanced magnetic resonance imaging and histology. *Circulation* 2005;112:3437-3444
21. Saam T, Ferguson MS, Yarnykh VL, Takaya N, Xu D, Polissar NL, et al. Quantitative evaluation of carotid plaque composition by in vivo MRI. *Arterioscler Thromb Vasc Biol* 2005;25:234-239

22. Lindsay AC, Biasiolli L, Lee JM, Kylintireas I, MacIntosh BJ, Watt H, et al. Plaque features associated with increased cerebral infarction after minor stroke and TIA: a prospective, case-control, 3-T carotid artery MR imaging study. *JACC Cardiovasc Imaging* 2012;5:388-396
23. Allkemper T, Tombach B, Schwindt W, Kugel H, Schilling M, Debus O, et al. Acute and subacute intracerebral hemorrhages: comparison of MR imaging at 1.5 and 3.0 T--initial experience. *Radiology* 2004;232:874-881
24. Zhu DC, Ferguson MS, DeMarco JK. An optimized 3D inversion recovery prepared fast spoiled gradient recalled sequence for carotid plaque hemorrhage imaging at 3.0 T. *Magn Reson Imaging* 2008;26:1360-1366
25. Ota H, Yarnykh VL, Ferguson MS, Underhill HR, Demarco JK, Zhu DC, et al. Carotid intraplaque hemorrhage imaging at 3.0-T MR imaging: comparison of the diagnostic performance of three T1-weighted sequences. *Radiology* 2010; 254:551-563
26. Wang J, Ferguson MS, Balu N, Yuan C, Hatsukami TS, Börnert P. Improved carotid intraplaque hemorrhage imaging using a slab-selective phase-sensitive inversion-recovery (SPI) sequence. *Magn Reson Med* 2010;64:1332-1340
27. Wasserman BA, Smith WI, Trout HH 3rd, Cannon RO 3rd, Balaban RS, Arai AE. Carotid artery atherosclerosis: in vivo morphologic characterization with gadolinium-enhanced double-oblique MR imaging initial results. *Radiology* 2002; 223:566-573
28. Clarke SE, Hammond RR, Mitchell JR, Rutt BK. Quantitative assessment of carotid plaque composition using multicontrast MRI and registered histology. *Magn Reson Med* 2003;50:1199-1208
29. Qiao Y, Ronen I, Viereck J, Ruberg FL, Hamilton JA. Identification of atherosclerotic lipid deposits by diffusion-weighted imaging. *Arterioscler Thromb Vasc Biol* 2007;27:1440-1446

경동맥 확산강조영상으로 증상이 있는 경동맥 죽종의 지방 풍부 괴사핵을 발견할 수 있는가?

이강지[1] · 곽효성[1,2]* · 정경호[1] · 황승배[1] · 송지수[1]

목적: 증상이 있는 경동맥 죽종의 지방 풍부 괴사핵을 발견하는 데 있어서 확산강조 자기공명영상 진단의 유용성을 조영증강 자기공명영상과 비교하여 알아보고자 하였다.

대상과 방법: 경동맥 플라크 자기공명영상의 조영증강 경동맥 자기공명 혈관조영술에서 중등도 이상의 경동맥 협착이 있고 증상이 있는 25명의 환자를 후향적으로 분석하였다. 에코 평면 확산강조영상의 자장세기를 b0, b200, b800, 그리고 b1000으로 주어 경동맥 플라크 자기공명영상을 얻었다. 두 명의 연구자가 확산강조영상에서 경화반이 보이는지를 협의하여 분석하였다. 또한 확산강조영상에서 다양한 자장세기값에 따른 경동맥 내강과 경화반 사이의 대도조 대 잡음비를 분석하였다.

결과: 8명의 환자가 경동맥 확산강조영상에서 경동맥 죽상경화반을 보였다. 16명의 환자는 경동맥 죽상경화반을 가지고 있다고 진단되었지만 확산강조영상에서는 보이지 않았다. 확산강조영상에서 보였던 집단은 그렇지 않은 집단과 비교하여 의미 있게 큰 최대 벽 두께와 세로 길이를 가진 죽상경화반을 보였다. b200 확산강조영상은 경동맥 내강과 지방 풍부 괴사핵 간에 가장 높은 대조도 대 잡음비를 나타내었다($p < 0.001$). 지방 풍부 괴사핵에 대한 b200 확산강조영상의 평균 겉보기 확산계수 값은 $0.51 \pm 1.55 \times 10^{-3}$ mm^2/s이었다.

결론: 경동맥 확산강조영상에서의 죽상경화반의 식별은 조영증강 자기공명영상과 비교하여 상대적으로 낮은 발견율을 보였다. 따라서 경동맥 확산강조영상은 지방 풍부 괴사핵을 포함한 경동맥 죽상경화반의 발견에 있어서 조영증강 자기공명영상을 대체할 수 없다.

[1]전북대학교 의학전문대학원 전북대학교병원 영상의학과, [2]전북대학교병원 임상의학연구소